Supplementary Information (SI) for Journal of Materials Chemistry A.
This journal is © The Royal Society of Chemistry 2025

Synergistic Linkage Engineering in Covalent Organic Frameworks for Boosting Photocatalytic Hydrogen Evolution

Changsheng Du[a,b] Tongtong Jia[b,c], Wenjing Na[b,d], Haojie Huang[a,b], Zewen You[a,b], Yunqi Liu[a,b], Wenjing Song[b,c], and Jianyi Chen*[a,b]

[a]Beijing National Laboratory for Molecular Sciences, Key Laboratory of Organic Solids, Institute of Chemistry, Chinese Academy of Sciences, Beijing 100190, PR China

[b]University of Chinese Academy of Sciences, Beijing 100049, PR China

[c]Key Laboratory of Photochemistry, CAS Research/Education Center for Excellence in Molecular Sciences

[d]Protein & Peptide Pharmaceutical Laboratory, Institute of Biophysics, Chinese Academy of Sciences, Beijing 100101, P.R. China

Correspondence and requests for materials should be addressed to J.C. (email: chenjy@iccas.ac.cn)

Table of contents

Section 1. Materials and methods

1. Materials and methods

Building blocks (Tta and Tfa) were obtained from CHEMSOON Co., Ltd, and pyruvic acid was obtained from Bide Pharmatech Co., Ltd. All other reagents and solvents were commercially available and used without further purification.

1.1 Powder X-ray diffraction

Powder X-ray diffraction (PXRD) patterns were recorded on PANalytical Empyrean diffractometer for Cu Kα radiation (α = 1.5406 Å) over the range of 2 θ = 2.0-30.0 with a step size of 0.02° and a scan speed of 3.5° min^{-1}.

1.2 Fourier-transform infrared spectroscopy

Fourier transform infrared (FT-IR) spectra were performed on a Bruker Optics Tensor-27 spectrometer in the range of 400-4000 cm^{-1}.

1.3 Solid nuclear magnetic resonance

The solid-state ^{13}C cross-polarization magic angle spinning (CP/MAS) NMR spectra were recorded on a Bruker NEO 600 WB spectrometer.

1.4 Thermogravimetric analysis

Thermogravimetric analysis (TGA) was carried out on a PerkinElmer series 7 thermal analysis system under N_2 by a heating rate of 10 ℃ min^{-1} within a temperature range of 50-800 ℃.

1.5 UV-visible absorption spectra

UV-visible absorption spectra were measured on a Lambda 1500+ UV-vis spectrometer by measuring the reflection of powders in the solid state.

1.6 X-ray photoelectron spectroscopy

X-ray photoelectron spectroscopy analysis (XPS) was performed on an ESCALAB250Xl spectrometer using Al Kα X-rays as the excitation source.

1.7 Fluorescence spectrophotometer

Fluorescence spectra were performed on a FluoroMax+.

1.8 Time-correlated single photo counting (TCSPC) measurements

TCSPC experiments were performed on an FLS980 spectrometer equipped with picosecond pulsed LED excitation sources and a R928 detector. An EPL-480 diode (λ

= 483.6 nm) with a 510 nm filter for emission detection was used. Solid samples were used directly for testing. Decay times were fitted in the FAST software using suggested lifetime estimates.

1.9 Electron paramagnetic resonance spectroscopy (EPR)

5 mg of TtaTfa-COF and QL-COF were separately added to nuclear magnetic tubes (5 mm o.d.) with caps. The EPR measurements were performed at 293 K by a Bruker Elexsys E500 spectrometer. The samples were illuminated by a 300 W Xe lamp with 400 nm cut-off filter. All the samples were measured under the same conditions (microwave power: 0.4 mW, microwave frequency ≈ 9.41 GHz, modulation frequency: 100 KHz, modulation amplitude: 3 G).

1.10 Transmission electron microscopy

Transmission electron microscopy (TEM) images were obtained on a Cryogenic Transmission electron microscopy (Cryo-TEM) Themis 300 operated at 200 kV. Scanning transmission electron microscopy (STEM) images were obtained on a JEOLJEM-F200 operated at 300 KV. All the samples were prepared by drop-casting sonicated ethanol suspensions of the materials onto a copper grid.

1.11 Scanning electron microscopy

Scanning electron microscopy (SEM) were obtained by S-4800 equipment.

1.12 Gas sorption analysis

Ar sorption isotherms were measured on a Quantachrome Autosorb-IQ Instrument at 87 K. Prior to the measurements, the samples were activated at 90 ℃ for 8 h before measuring under vacuum. The surface areas were calculated from the adsorption data using Brunauer-Emmett-Teller (BET) model. The pore-size-distribution curves were obtained using non-localized density functional theory (NLDFT).

1.13 Water vapour sorption

Water vapour sorption experiment was conducted on a micromeritics 3Flex. Samples were pretreated under vacuum at 90 ℃ for 8 h. The water adsorption isotherms were performed at 298 K.

1.14 Elemental analysis

Elemental analysis was carried out on an organic elemental analyzer (Thermo Flash

Smart).

1.15 Transient absorption measurements

Femtosecond Transient (TA) absorption spectra were measured by Vitara T-Legend Elite-TOPAS-Helios-EOS-Omni. Light pulses were provided from a Ti: Sa amplified laser system (Legend Elite-1K-HE). Wavelengths of pump light were 365 nm, while the wavelength range of the detected is 385-700 nm.

1.16 Electrochemical measurements

These measurements were performed with an electrochemical workstation (Autolab, PGSTAT 302 N, Metrohm) using a three-electrode cell system under irradiation of a 300 W Xe lamp (CEL-HXF300). The ITO glass (1×2 cm^2) coated materials as the photoelectrode, a Pt foil as the counter electrode, and an Ag/AgCl electrode as the reference electrode, respectively. ITO glasses were washed with acetone, ethanol and isopropanol for several times. The working electrode was prepared as follows: 2 mg COF powder was dispersed in 2 mL ethanol and water (v:v = 1:1), followed by ultra-sonicated for 1 h to get a homogeneous slurry. After the addition of 20 μL Nafion, the mixture was spread onto ITO glass to get a regular membrane with defined area. The three electrodes were inserted in a quartz cell filled with 0.1 M Na_2SO_4 electrolyte. The Na_2SO_4 electrolyte was purged with N_2 for 1 h prior to the measurements. The electrochemical impendence measurements were carried out under the open-circuit condition in the frequencies range of 0.1 Hz to 10^4 Hz. The transformation of NHE and Ag/AgCl electrode is showed below (the electrochemical potential at pH = 7):

$$E(vs.NHE) = E(vs.Ag/AgCl) + 0.1976$$

1.17 Photocatalytic hydrogen evolution test

In a typical photo-reaction, 3 mg COF was dispersed in 30 mL H_2O containing 0.1 M ascorbic acid and 2 wt% Pt (10 μL K_2PtCl_6 aqueous solution, 0.03 M). Prior to irradiation, the reaction mixture was purged by Ar to remove air in the reaction. Then, the photocatalytic reaction was carried out with a 300 W Xe lamp at $\lambda > 400$ nm and the incident intensity was c.a.200 mW cm^{-2}. The reaction temperature was kept at 20 ± 0.2 ℃ by circulating water system. The gaseous product was taken from the headspace and H_2 was monitored by gas chromatography (Fuli GC-2060) equipped with a thermal

conductive detector (TCD) and a packed column (TDX-01) with a sampling (0.2 mL) under the specified time. Hydrogen dissolved in the reaction mixture was not measured and the pressure increase generated by the evolved hydrogen was neglected in the calculations. The amount of evolved H_2 were determined from a linear regression fit. The cycling stability of COF was using the same way after samples were collected and washed with water, then by direct dispersion in the next catalytic run without adding extra Pt source. This process was repeated for four times.

1.18 The apparent quantum efficiency measurement

The apparent quantum efficiency (AQY) for the photocatalytic H_2 evolution was measured at monowavelength λ = 420, 450, and 520 nm LED (100 mW cm^{-2}). An area of 17.59 cm^2 was illuminated. The AQY were estimated using the equation below:

$$\eta_{EQE} = 2 \times \frac{moles\ of\ hydrogen\ evolved}{moles\ of\ the\ incidentphotos} \times 100\%$$

1.19 Density functional theory calculations

1) Water adsorption energy calculations. We have employed the Vienna Ab Initio Package (VASP)[1, 2] to perform all density functional theory (DFT) calculations within the generalized gradient approximation (GGA) using the Perdew-Burke-Ernzerhof (PBE)[3] formulation. We have chosen the projected augmented wave (PAW) potentials[4, 5] to describe the ionic cores and take valence electrons into account using a plane wave basis set with a kinetic energy cutoff of 450 eV. Partial occupancies of the Kohn−Sham orbitals were allowed using the Gaussian smearing method and a width of 0.05 eV. The electronic energy was considered self-consistent when the energy change was smaller than 10^{-5} eV. A geometry optimization was considered convergent when the energy change was smaller than 0.02 eV $Å^{-1}$. The weak interaction was described by DFT+D3 method using empirical correction in Grimme's scheme.[6, 7]

The adsorption energy (E_b) has been calculated using Eq. 1,

$E_{ads} = E_{total} - E_{substrate} - E_{H2O}$ (1)

The E_{total}, $E_{substrate}$ and E_{H2O} represent the energy of the COF with H_2O, COF bulk and H_2O molecule in adsorption structure, respectively.

2) The excited states calculations. All-electron DFT calculations have been carried

out by the ORCA quantum chemistry software[8] (Version 5.0.3). For geometry optimization calculations, BLYP functional and the def2-SV(P) basis set[9] were used, and the optimal geometry for each compound was determined. The excited states calculations were performed with B3LYP functional and the def2-SVP basis set.[10] The DFT-D3 dispersion correction with BJ-damping[6, 7] was applied to correct the weak interaction to improve the calculation accuracy. Hole-electron analysis is performed by Multiwfn package.[11]

1.20 Preparation of TtaTfa-COF.

2,4,6-Tris(4-aminophenyl) triazine (Tta, 20 mg, 0.056 mmol) and 1,3,5-Tris(4-formylphenyl) amine (Tfa, 18.6 mg, 0.056 mmol) were filled into a reaction tube, followed by the addition of mesitylene (0.5 mL) and dioxane (0.5 mL). The mixture was sonicated for 10 minutes. 6 M acetic acid (0.1 mL) was added to the mixture and further sonicated for another 5 minutes. The tube was degassed by the three freeze-pump-thaw cycles and was then sealed. Upon warming to room temperature, the sealed tube was heated at 120 ℃ for 3 days. The resultant precipitate was filtrated, washed with tetrahydrofuran (THF), activated by Soxhlet extraction using THF overnight and further washed with water. Finally, the solid was collected and dried at 90 ℃ under vacuum for 24 h to give a product with an isolated yield of 72 %.

1.21 Synthesis of QL-COF.

TtaTfa-COF (30 mg) was first dispersed into 2 mL mesitylene and stirred for 5 minutes. Then pyruvic acid (2 equivalents per imine bonds) was added to the above mixture, followed by stirred and warming up to 100 ℃ for 6 h. Upon cooling to room temperature, the resulting powder was collected by filtration and washed with THF, acetone, and EtOH. Subsequently, the powder was subjected to Soxhlet extraction using THF for 24 h and dried at 90 ℃ under vacuum to give a product with an isolated yield 73 %.

Section 2. Characterization figures and photocatalytic data

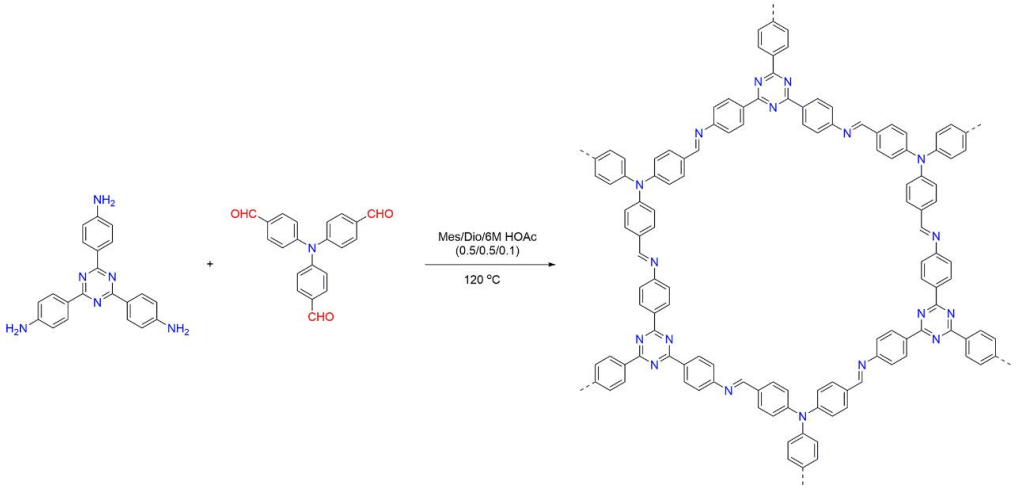

Figure S1. The synthesis of TtaTfa-COF.

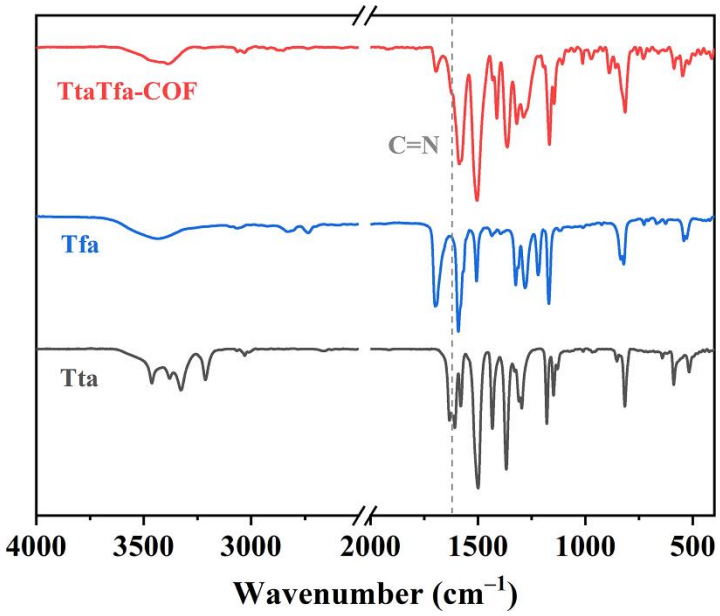

Figure S2. FT-IR spectra of TtaTfa-COF and its monomers.

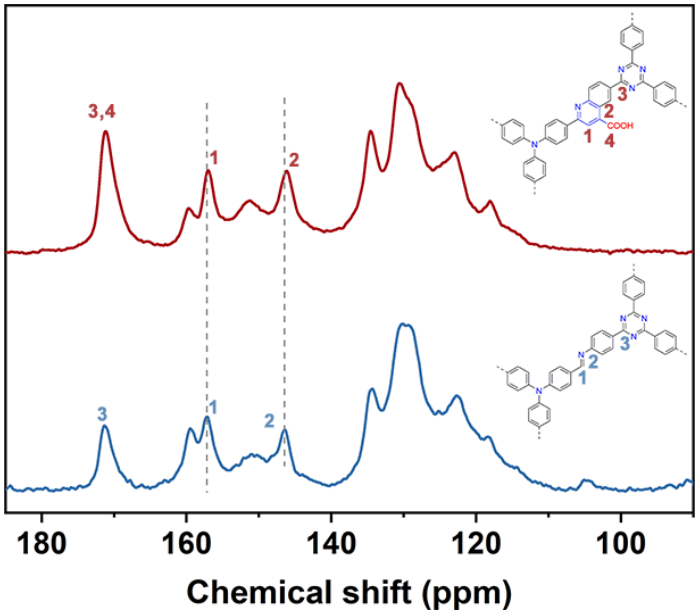

Figure S3. Solid-state ^{13}C CP-MAS NMR spectra of TtaTfa-COF and QL-COF.

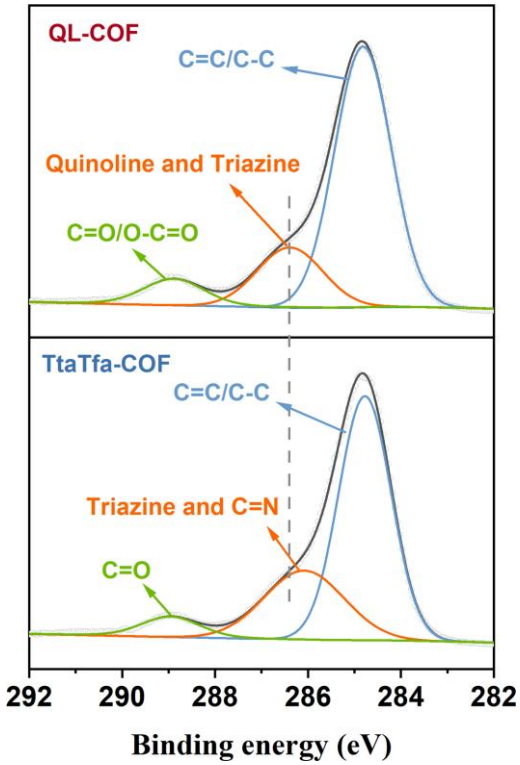

Figure S4. C 1s XPS spectra of TtaTfa-COF and QL-COF. After cyclization, the binding energy of imine bond shifted from 286.08 eV to 286.43 eV. In addition, the relative intensity of C=O signals enhanced due to the introduction of $–CO_2H$ groups in QL-COF.

Table S1. Elemental analysis of TtaTfa-COF and QL-COF.

COFs		C (%)	H (%)	N (%)
TtaTfa-COF	Calcd.	80.13	4.29	15.58
	Found	77.91	4.44	14.88
QL-COF	Calcd.	73.47	3.24	11.76
	Found	71.51	4.60	11.35

Experimental results reveal that the C, H, N contents are close to the calculated values. The slight deviation may result from the unreacted edge groups or defects in the extended frameworks.

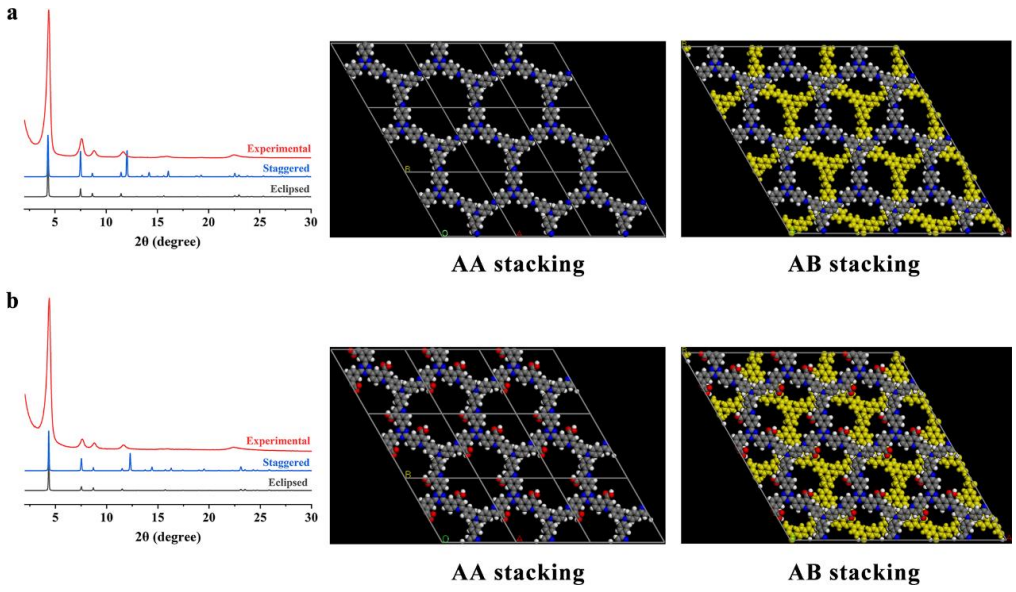

Figure S5. PXRD patterns and simulated structural models of (a) TtaTfa-COF and (b) QL-COF.

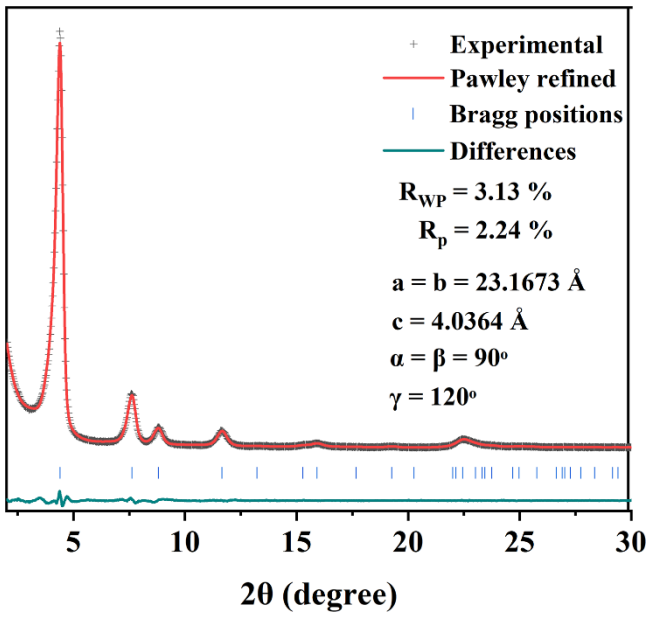

Figure S6. Experimental PXRD pattern of TtaTfa-COF.

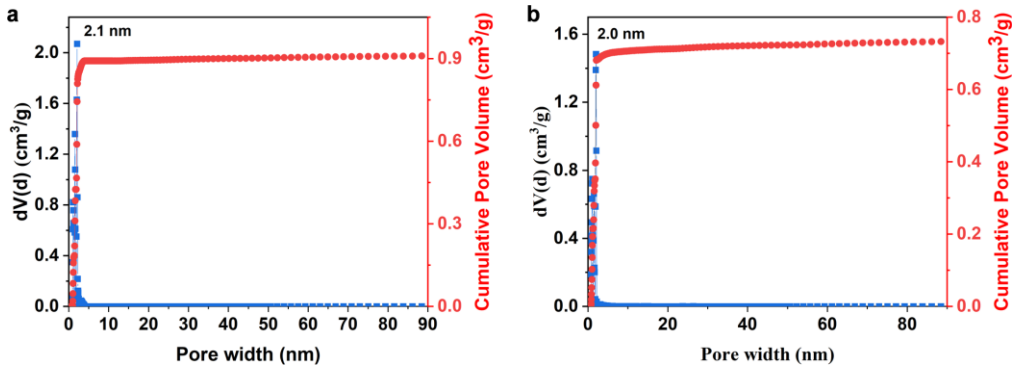

Figure S7. Pore size distribution of (a) TtaTfa-COF and (b) QL-COF.

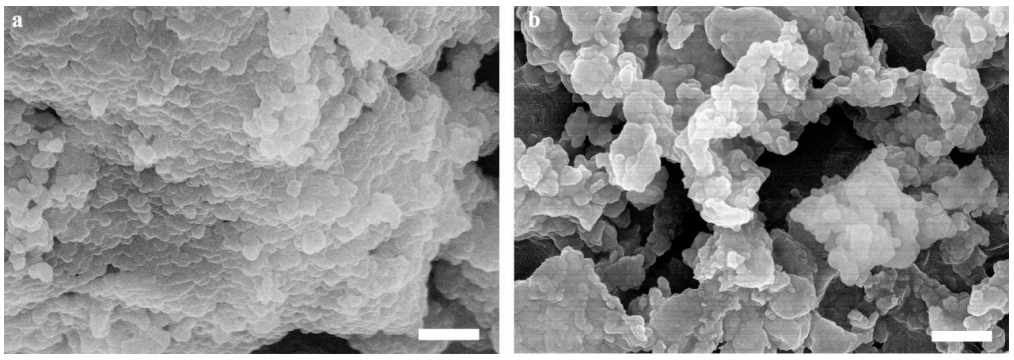

Figure S8. SEM images of (a) TtaTfa-COF and (b) QL-COF. Scale bar 500 nm.

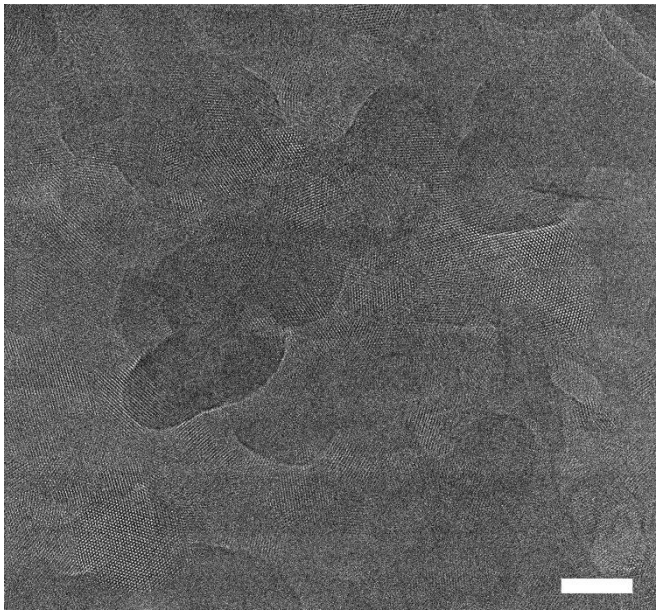

Figure S9. TEM images of TtaTfa-COF. Scale bar 50 nm.

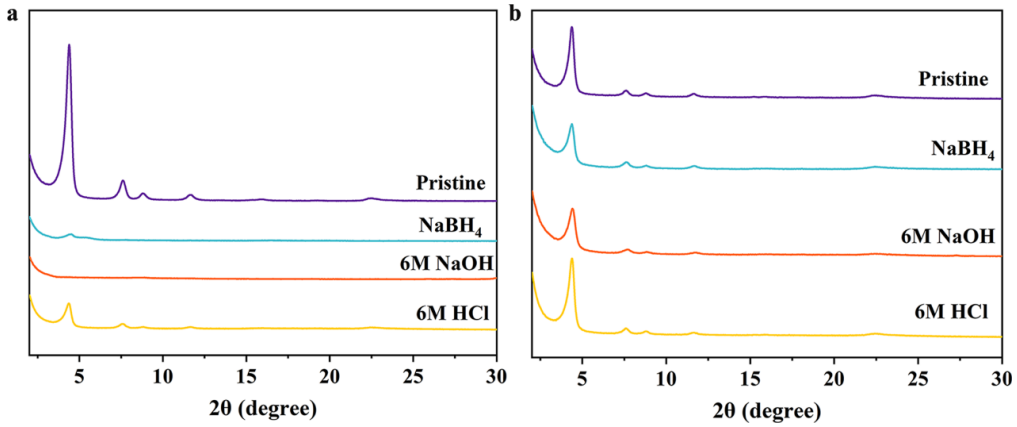

Figure S10. PXRD patterns of (a) TtaTfa-COF and (b) QL-COF after treatment under harsh chemical conditions for 2 days.

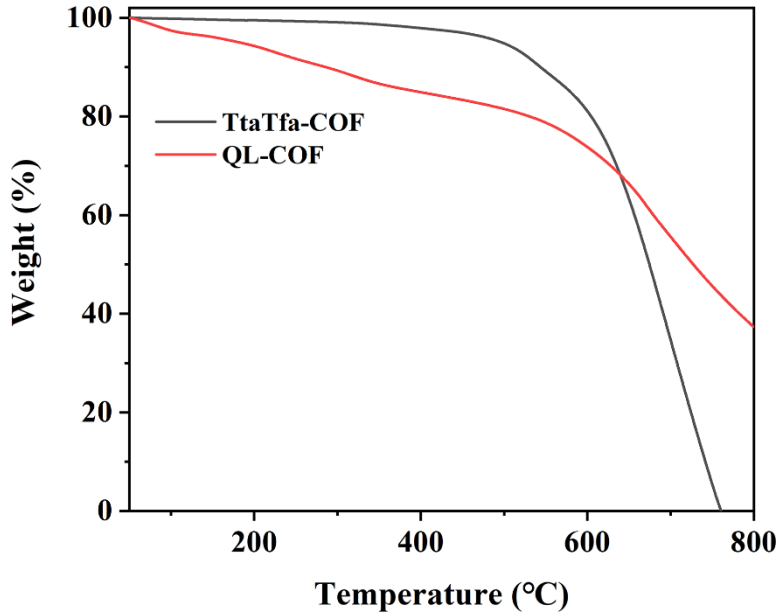

Figure S11. TGA of TtaTfa-COF and QL-COF.

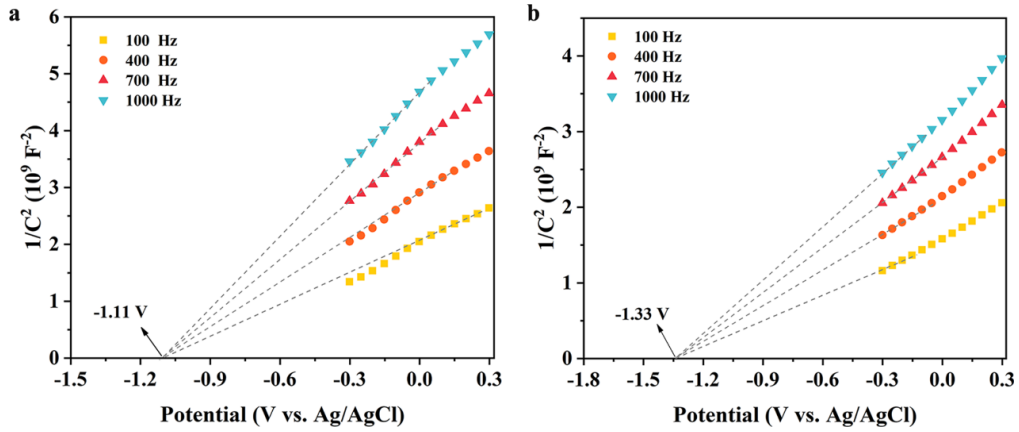

Figure S12. Mott-Schottky plots of (a) TtaTfa-COF and (b) QL-COF. The flat (conduction) band potentials of TtaTfa-COF and QL-COF (*E* vs. Ag/AgCl) measured are − 1.11 V and − 1.33 V, respectively when the ITO glass (1×2 cm^2) coated COFs as the photoelectrode, a Pt foil as the counter electrode, and an Ag/AgCl electrode as the reference electrode. These values can be converted to potentials relative to the standard hydrogen electrode (− 0.91 V for TtaTfa-COF and − 1.13 V for QL-COF) using the formula below.

$$E(vs.NHE) = E(vs.Ag/AgCl) + 0.1976$$

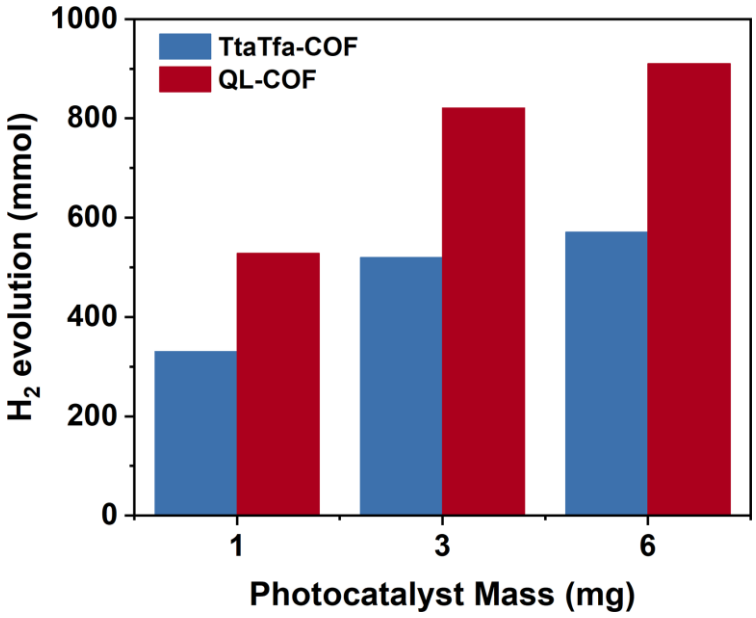

Figure S13. Dependence of the amount of H_2 evolution for TtaTfa-COF and QL-COF with different mass.

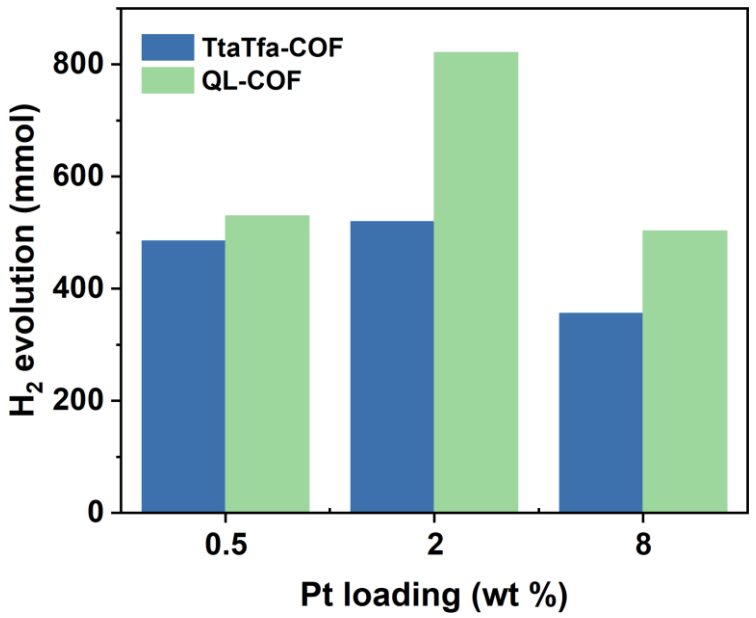

Figure S14. Dependence of the amount of H_2 evolution for TtaTfa-COF and QL-COF with different Pt loading amount.

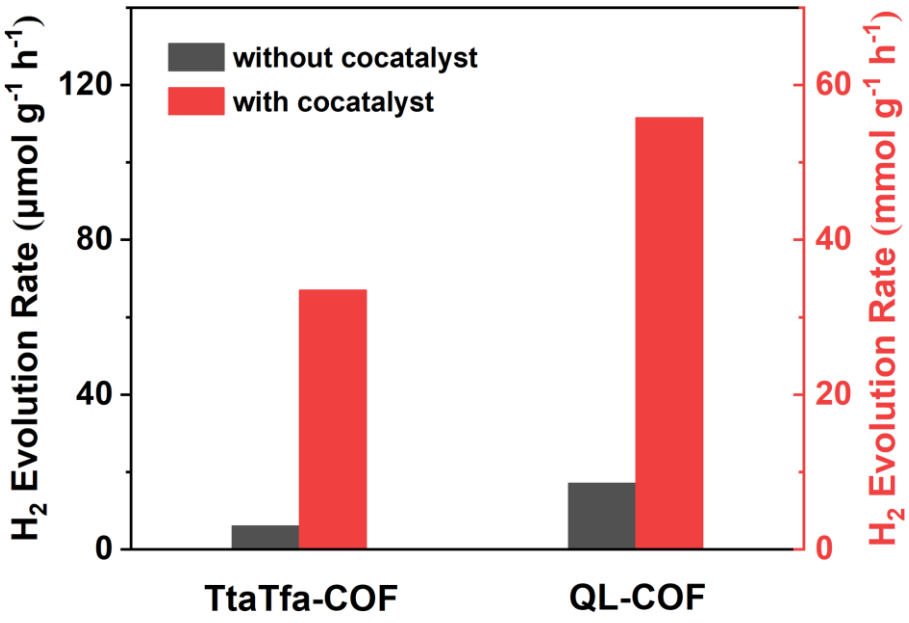

Figure S15. The photocatalytic performances of TtaTfa-COF and QL-COF with and without co-catalyst (Pt) under visible light (λ > 400 nm) irradiation.

We have conducted some control experiments to evaluate the photocatalytic effect under conditions without catalysts, co-catalysts, or sacrificial agents. The results of the control experiments indicate that no hydrogen was detected in the absence of COFs or the sacrificial agent. Moreover, the photocatalytic hydrogen production ability of the system was poor when the cocatalyst Pt was absent. These results demonstrate the indispensability of COF, the cocatalyst, and the sacrificial agent in the reaction system.

Table S2. The HER comparison of TtaTfa-COF and QL-COF with other representative COF-based photosensitizers.

Entry	Co-catalyst	Condition	Light source	HER (mmol $g^{-1}h^{-1}$)	AQY (%)	Ref
QL-COF	Pt (2 wt %)	AA	> 400 nm	55.83	1.85 (450 nm)	**This work**
TtaTfa-	Pt	AA	> 400	33.54	1.42	**This work**

COF	(2 wt %)		nm		(450 nm)	
TAPPy-DBTDP-COF	Pt (6 wt %)	AA	> 420 nm	12.7	5 (450 nm)	*Adv. Energy Mater.* 2024, **14**, 2402395.
Exfo-TTB-PT	Pt (3 wt %)	AA	> 300 nm	27.24	1.25 (475 nm)	*J. Mater. Chem. A,* 2024, **12**, 1292–1299
COF-JLU35	Pt (1 wt %)	AA	> 420 nm	70.8	3.21 (500 nm)	*J. Am. Chem. Soc.* 2023, **145**, 8364–8374
COF-JLU100	Pt (1 wt %)	AA	> 420 nm	87.6	5.13 (450 nm)	*Angew. Chem. Int. Ed.* 2022, **61**, e202208919
BTH-3	Pt (8 wt %)	AA	> 420 nm	15.1	1.25 (500 nm)	*Nat. Commun.* 2022, **13**, 100
Sono COF-3	Pt (4 wt %)	AA	> 420 nm	16.6	3.71 (420 nm)	*Nat. Synth.* 2022, **1**, 87
Py-ClTP-BT-COF	Pt (5 wt %)	AA	> 420 nm	8.875	8.45 (420 nm)	*Angew. Chem. Int. Ed.* 2020, **59**, 16902–16909
FS-COF	Pt (3.8 wt %)	AA	> 420 nm	10.1	3.20 (420 nm)	*Nat. Chem.* 2018, **10**, 1180-1189
g-$C_{18}N_3$-COF	Pt (3 wt %)	AA	> 420 nm	0.292	1.06 (420 nm)	*J. Am. Chem. Soc.* 2019,

						141, 14272
TP-BDDA-COF	Pt (3 wt %)	TEOA	> 395 nm	0.324	1.80 (520 nm)	*J. Am. Chem. Soc.* 2018, **140**, 1423−1427

Note: AA = ascorbic acid, TEOA = triethanolamine.

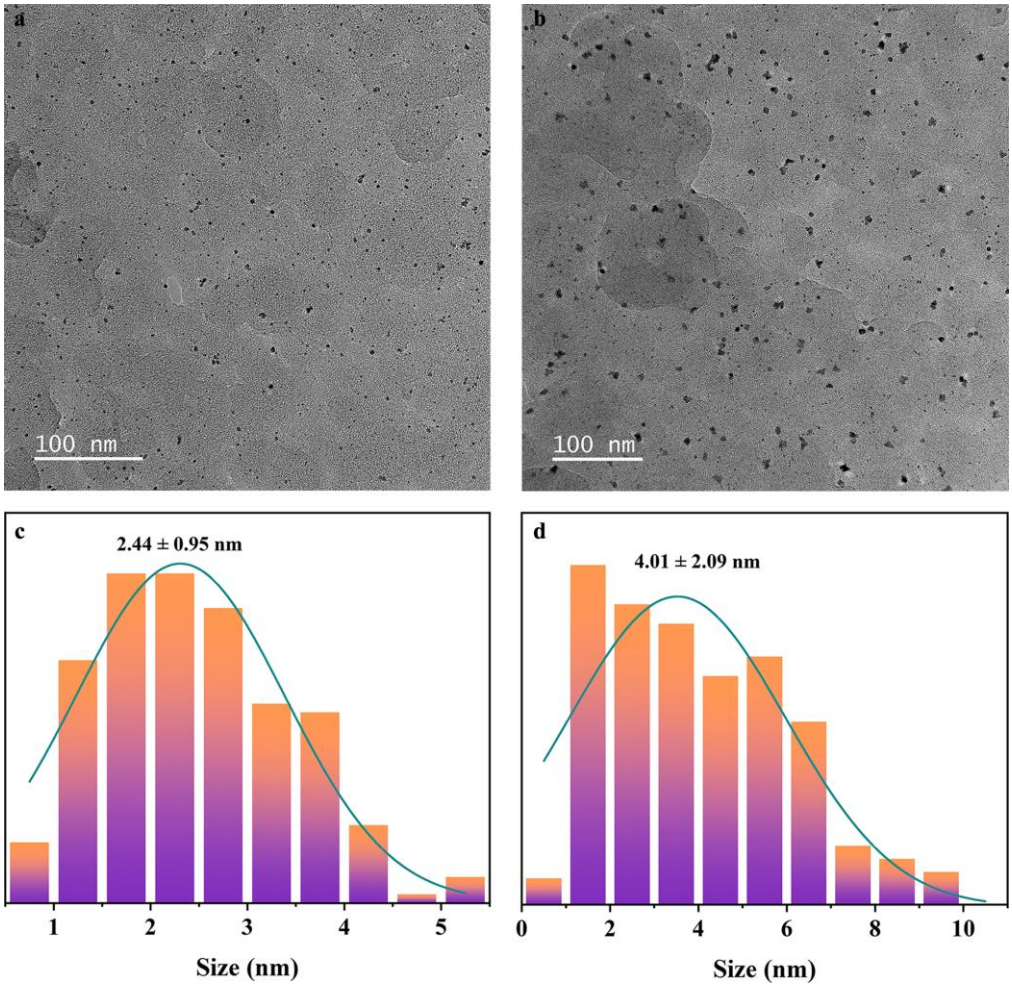

Figure S16. STEM images of (a) TtaTfa-COF and (b) QL-COF. Size distributions of Pt nanoparticles on (a) TtaTfa-COF and (b) QL-COF.

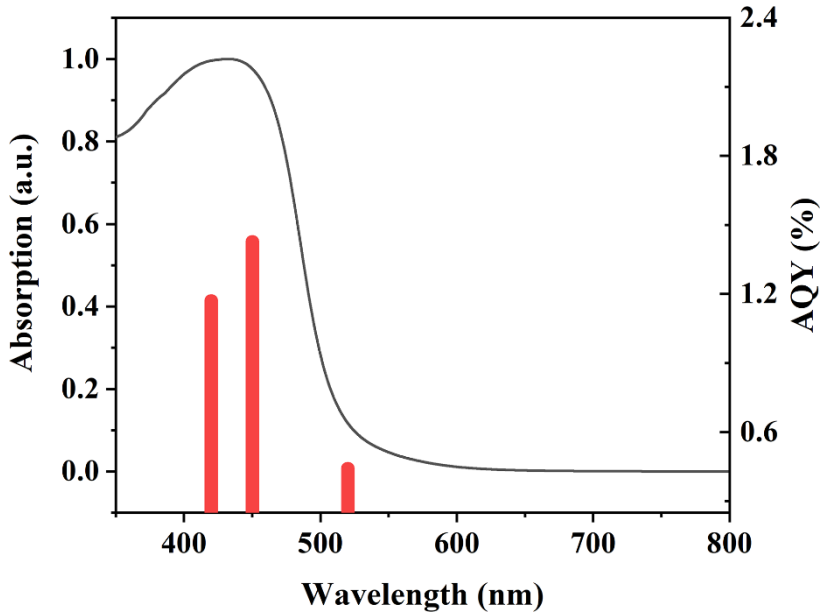

Figure S17. Wavelength-dependent AQY of photocatalytic hydrogen evolution by TtaTfa-COF photocatalyst.

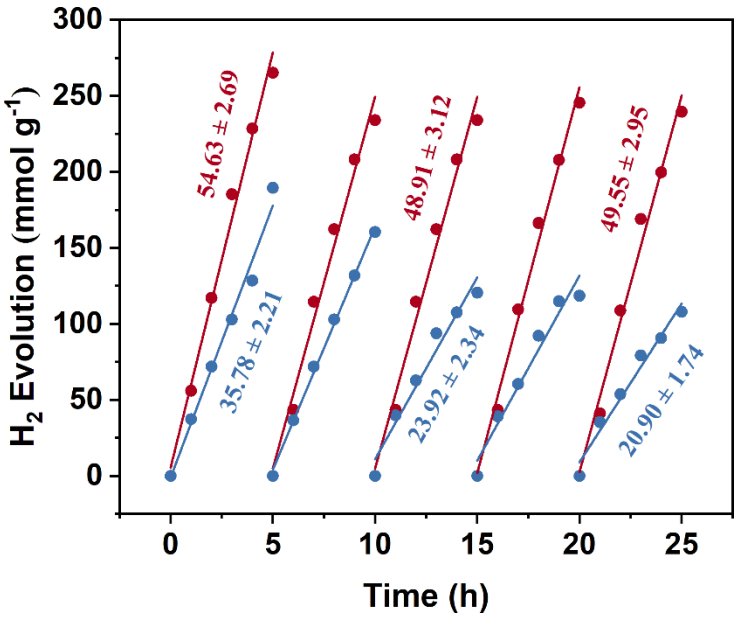

Figure S18. Time course hydrogen evolution curve of TtaTfa-COF and QL-COF. QL-COF can maintain a stable photocatalytic hydrogen evolution rate within five cycles, whereas the hydrogen evolution rate of TtaTfa-COF markedly declines within the same period.

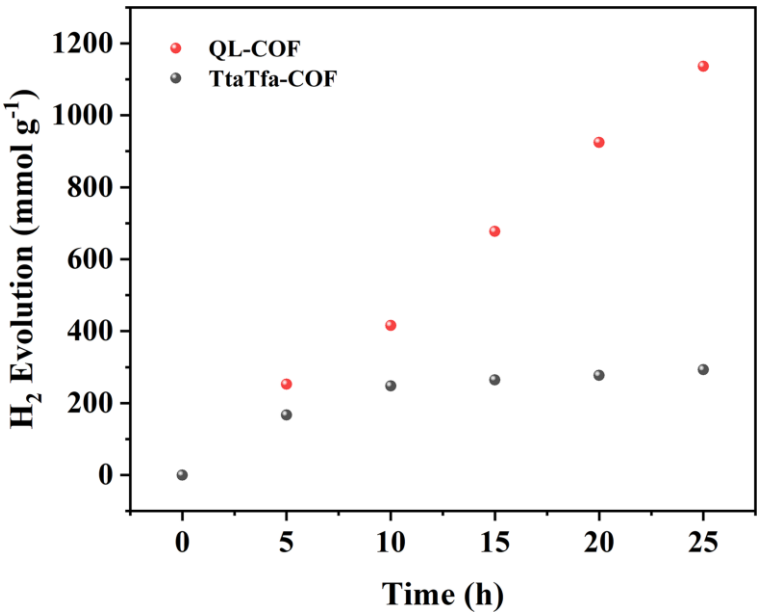

Figure S19. Longer-term hydrogen evolution experiments for TtaTfa-COF and QL-COF with a single cycle.

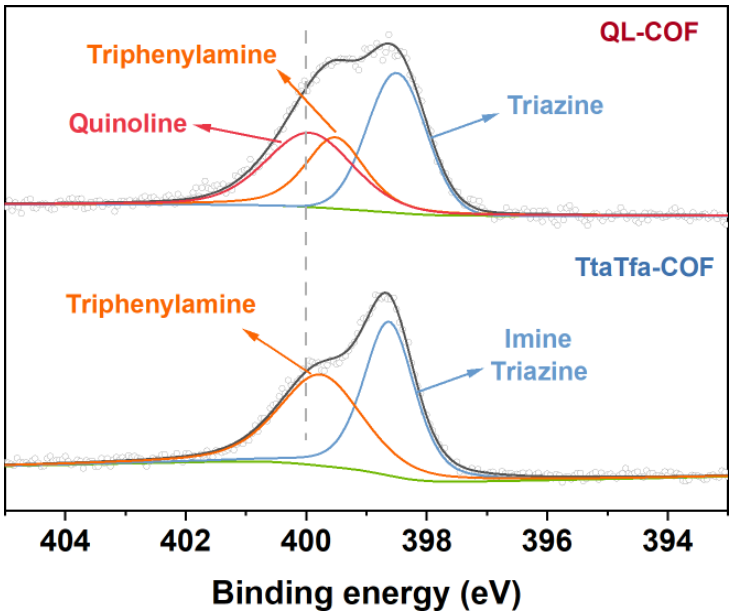

Figure S20. XPS spectra of N 1s in TtaTfa-COF and QL-COF after 25 h of reaction.

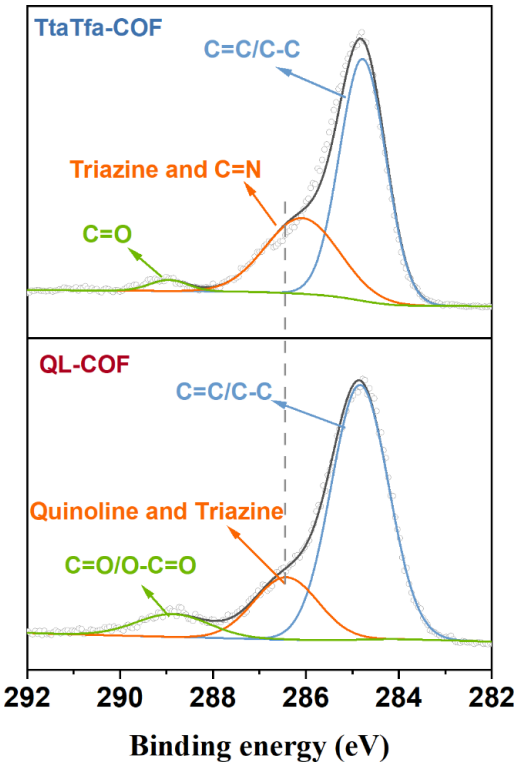

Figure S21. XPS spectra of C 1s in TtaTfa-COF and QL-COF after 25-hour reaction.

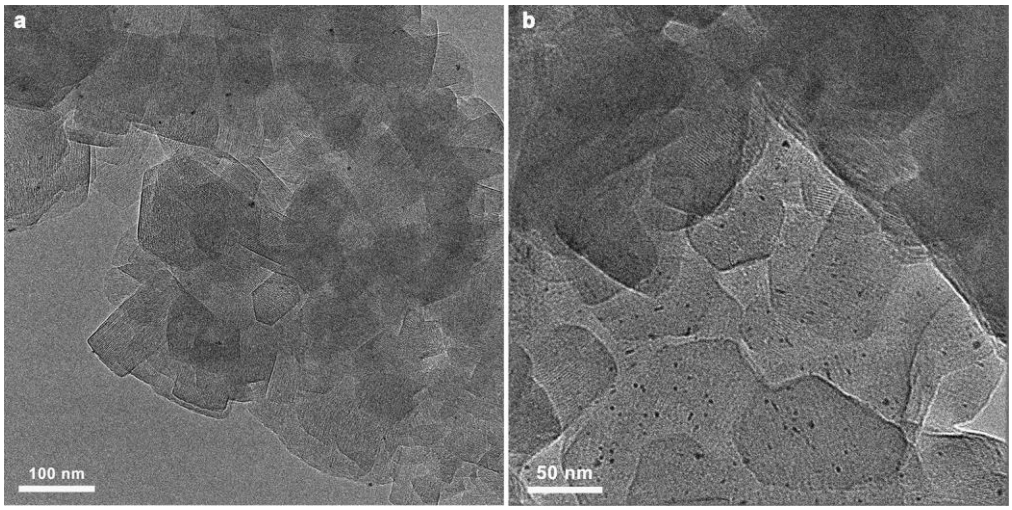

Figure S22. HRTEM images of (a) TtaTfa-COF and (b) QL-COF after 25-hour reaction.

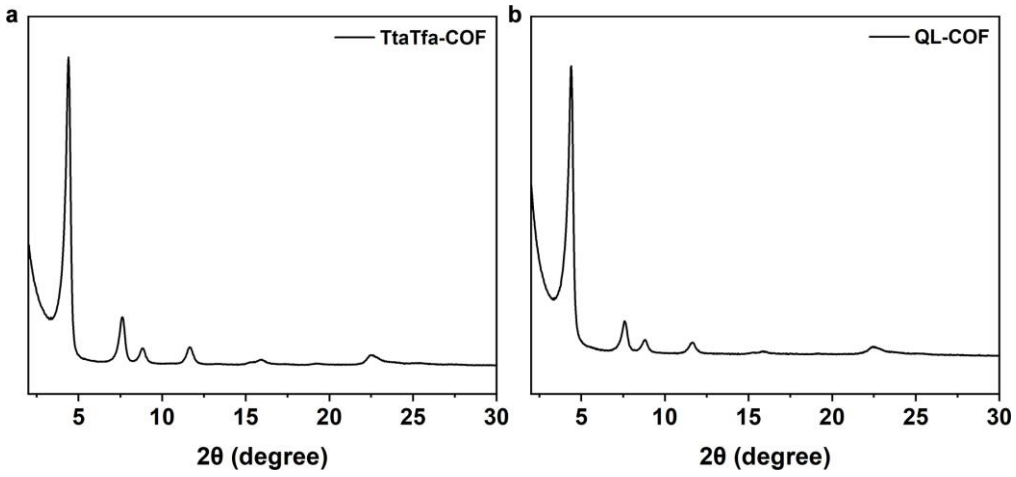

Figure S23. PXRD patterns of (a) TtaTfa-COF and (b) QL-COF after 25-hour reaction.

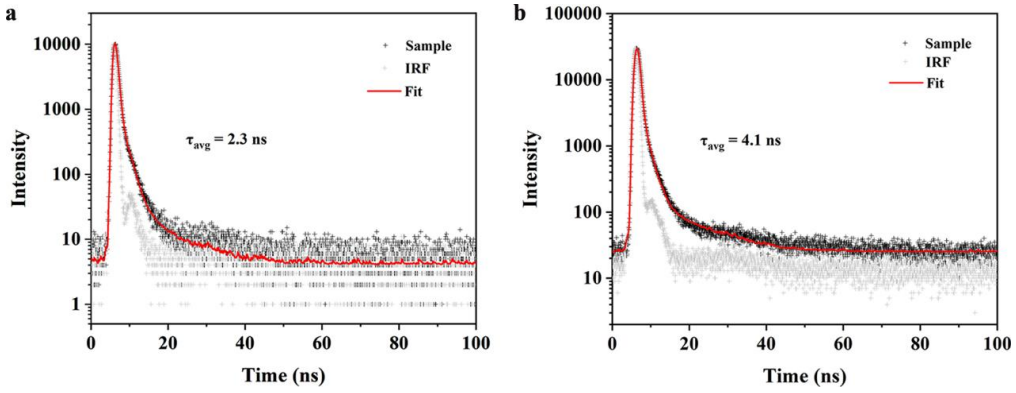

Figure S24. Time-resolved fluorescence spectra of (a) TtaTfa-COF and (b) QL-COF.

Section 3. References

References

1. G. Kresse and J. Furthmüller, *Comput. Mater. Sci.*, 1996, **6**, 15-50.
2. G. Kresse and J. Furthmüller, *Phys. Rev. B*, 1996, **54**, 11169-11186.
3. J. P. Perdew, K. Burke and M. Ernzerhof, *Phys. Rev. Lett.*, 1996, **77**, 3865-3868.
4. G. Kresse and D. Joubert, *Phys. Rev. B*, 1999, **59**, 1758-1775.
5. P. E. Blöchl, *Phys. Rev. B*, 1994, **50**, 17953-17979.
6. S. Grimme, J. Antony, S. Ehrlich and H. Krieg, *J. Chem. Phys*, 2010, **132**, 154104.
7. S. Grimme, S. Ehrlich and L. Goerigk, *J. Comput. Chem.*, 2011, **32**, 1456-1465.

8. F. Neese, *WIREs Comput. Mol. Sci.*, 2022, **12**, e1606.

9. F. Weigend and R. Ahlrichs, *Phys. Chem. Chem. Phys.*, 2005, **7**, 3297-3305.

10. D. Aravena, F. Neese and D. A. Pantazis, *J. Chem. Theory Comput.*, 2016, **12**, 1148-1156.

11. T. Lu and F. Chen, *J. Comput. Chem.*, 2012, **33**, 580-592.